Surface Science 115 (1982) 553–568
North-Holland Publishing Company

THEORETICAL STUDIES OF CO/Ni(100): GEOMETRY, VIBRATIONAL FREQUENCIES AND IONIZATION POTENTIALS FOR THE ON-TOP SITE

Janet N. ALLISON and William A. GODDARD III

*Arthur Amos Noyes Laboratory of Chemical Physics *, California Institute of Technology, Pasadena, California 91125, USA*

Received 10 August 1981

The chemisorption of CO on the (100) surface of Ni has been studied using an Ni_{14} cluster and generalized valence bond (GVB) methods. CO is found to bond perpendicular to the Ni surface with optimized Ni–C and C–O bond distances of 1.94 and 1.15 Å, respectively. The calculated Ni–CO bond strength is 29.7 kcal (experimental values 30–32 kcal). Vibrational frequencies are calculated to be 401 cm^{-1} for Ni–C stretch, 327 cm^{-1} for NiCO bend, and 2129 cm^{-1} for CO stretch. This decrease of the CO frequency by 71 cm^{-1} from the free molecule value is consistent with experiment based on self-consistent calculations of the positive ion states. We propose a new explanation for the loss of one PES peak upon chemisorption.

1. Introduction

The adsorption of CO onto nickel surfaces has been the subject of numerous studies over the past few decades. This is a key step in methanation,

$$3\,H_2 + CO \rightarrow CH_4 + H_2O,$$

and in Fischer–Tropsch synthesis. Although Auger data and CO flash desorption results show a 10–20% monolayer of carbide-like carbon on the active catalyst following the reaction [1], the overall mechanism (detailed sequence of reaction steps) is not understood.

In this paper we focus on the physical properties of adsorption of molecular CO at the on-top site of the Ni(100) surface.

The properties of the bare Ni_{14} cluster are described in section 2 and the bonding of CO onto this cluster is discussed in section 3. Finally, the vibrational frequencies and ionization potentials are analyzed and compared with experimental results.

* Contribution No. 6501.

0039-6028/82/0000–0000/$02.75

2. The Ni_{14} cluster

Previous studies of CO on Ni(100) suggest that the binding of CO is one-coordinate (on-top) [2,3], two-coordinate (bridged) [4], or a mixture of

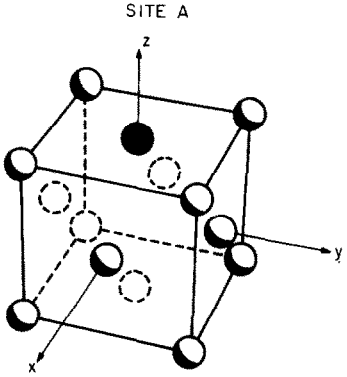

Fig. 1. The Ni_{14} cluster (5:4:5), Oh symmetry. Site A is the bonding site.

both terminal and bridged sites [5,6]. Andersson [6] interprets peaks in electron energy loss spectra (EELS) at 239 and 256 meV for a dilute CO lattice gas on Ni(100) to be due to bridging CO (two-coordinate) and on-top CO (one-

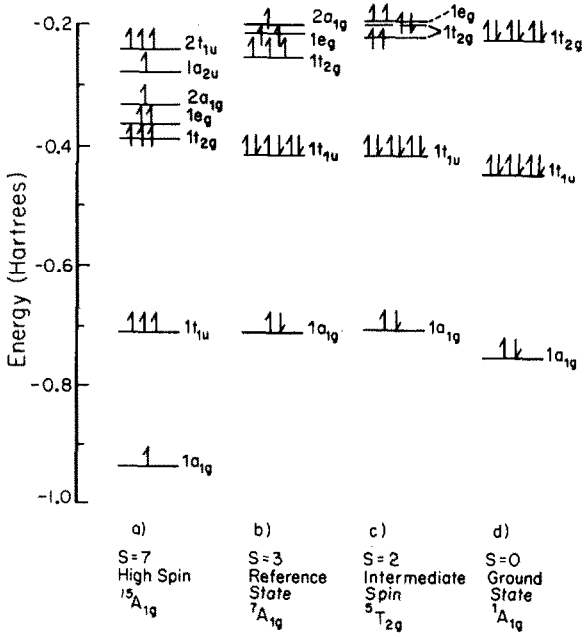

Fig. 2. Orbital energies for various spin states of Ni_{14}.

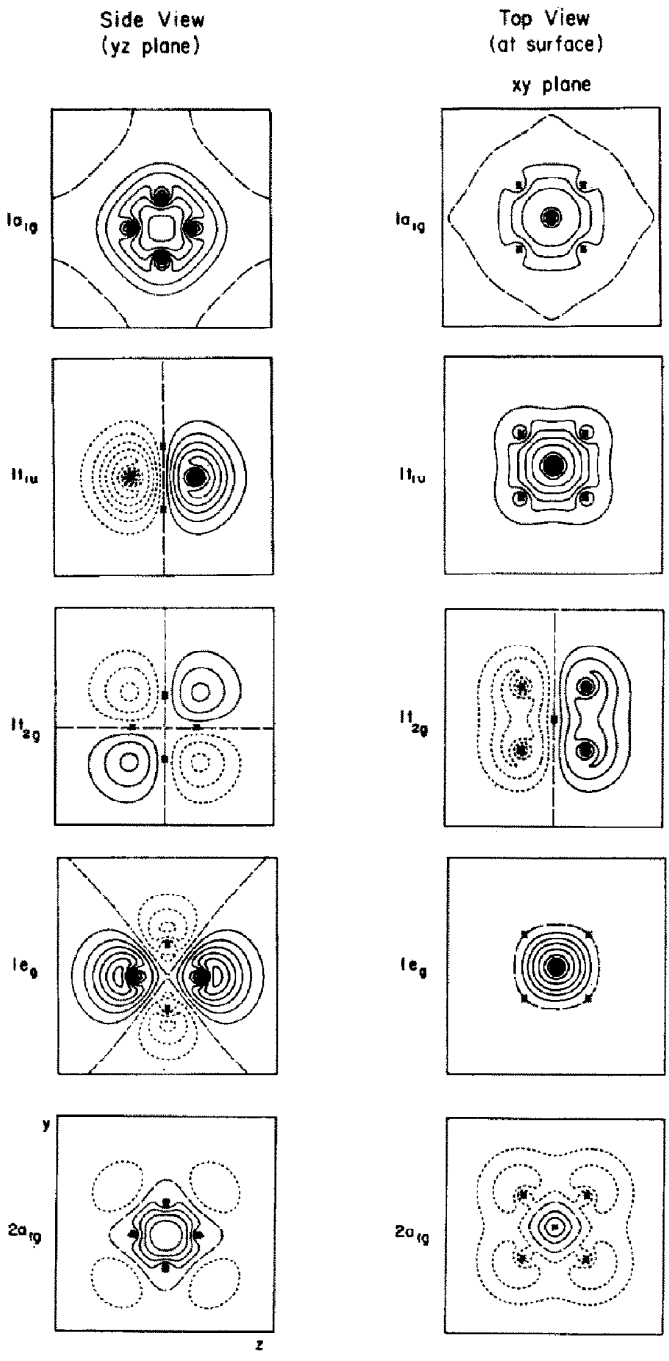

Fig. 3. Occupied band orbitals from the $^7Ag_{1g}$ state.

Table 1
Low-lying states of Ni_{14}

State		$1a_{1g}$	$1t_{1u}$			$1t_{2g}$		
			x	y	z	xy	xz	yz
High spin	$^{15}A_{2u}$	1	1	1	1	1	1	1
Reference state	$^{7}A_{1g}$	2	2	2	2	1	1	1
Intermediate spin	$^{5}T_{2g}$	2	2	2	2	2	1	1
	$^{3}T_{1g}$	2	2	2	2	1	2	2
Ground state	$^{1}A_{1g}$	2	2	2	2	2	2	2

coordinate), respectively. However, at higher coverages only a single peak at 256 meV is observed, indicating that the on-top species is the only one present. In order to model the bonding at the on-top site, we use the 14-atom cluster shown in fig. 1. The atoms are at the corners and face centers of a cube, just as in the cubic unit cell of the face centered cubic (fcc) structure. The CO is bonded to an atom at a face center (site A of fig. 1). This cluster contains all eight metal atoms that are nearest neighbors to the bonding site plus additional atoms such that there are three layers in all three directions. As in previous calculations of Ni clusters, all calculations were fully self-consistent wavefunctions using proper open-shell formalisms [7]. In calculating an excitation energy or ionization potential, full SCF calculations are done on both states (we do *not* use Koopmans' Theorem). The Ar core of Ni was replaced by an effective potential [8] through a fit to an ab initio description of Ni atom and subsequently modified [9] to include a spherically averaged potential for the $3d^9$ configuration of Ni. A double zeta (DZ) basis was used to describe the remaining 4s orbital [10].

In order to provide some feel for the electronic structure of Ni_{14}, we show four sets of energy levels in fig. 2. Fig. 2a is for the case with maximum spin ($S = 7$) for the 14 electrons in the conduction band (useful in predicting the configurations for low-lying states of Ni_{14}). Based on this diagram, it is clear that the $1a_{1g}$ and t_{1u} orbitals should be doubly-occupied. With these orbitals doubly-occupied, the maximum spin is $S = 3$, leading to the optimum configuration in fig. 2b with singly-occupied orbitals t_{2g}, e_g, and $2a_{1g}$. All the low-lying states of Ni_{14} involve distribution of the electrons over these orbitals, as indicated in table 1. These orbitals are shown in fig. 3.

The ground state of Ni_{14} is the singlet state, $^{1}A_{1g}$. The ionization potential (approximate work function) for this state is calculated to be 6.07 eV (Koopmans' Theorem gives 6.15 eV), which is slightly larger than the work function for nickel, 5.2 eV. The delocalized orbitals of the Ni_{14} cluster occupied by the 4s electrons have "conduction band" character, and the orbital energy spectrum produced by the $^{1}A_{1g}$ ground state of the cluster is shown in fig. 2d. These

e_g		$2a_{1g}$	$2t_{1u}$			a_{2u}	Total energy	Excitation energy
z^2	x^2-y^2		x	y	z	xyz	(h)	(eV)
1	1	1	1	1	1	1	−3.3502	0.844
1	1	1	0	0	0	0	−4.3097	0.259
1	1	0	0	0	0	0	−4.2933	0.705
0	1	0	0	0	0	0	−4.2973	0.596
0	0	0	0	0	0	0	−4.3192	0

orbital energies define a bandwidth of 12.7 eV. The calculated electron affinity is 1.81 eV. As discussed elsewhere [11], the electron affinity is much lower than the bulk value.

3. CO chemisorbed on Ni_{14}

3.1. Geometries and energies

In describing the interaction of CO with an Ni surface, it is essential to describe the charge distribution of CO properly. It is well known [12–14] that even the exact uncorrelated wavefunction (Hartree–Fock) gives the wrong sign for the dipole moment of CO, and hence we have used correlated wavefunctions, generalized valence bond (GVB). The problem with the Hartree–Fock (HF) wavefunction is the lack of correlation in the π bonds. Including just this correlation in the two π bonds [GVB(2/4)] leads to a dipole moment of 0.124 D, in excellent agreement with the experimental value $\mu = 0.122$ D [15]. Dependence of the dipole moment upon electron correlation and upon basis set is shown in table 2. There we see that GVB(2/4) with a DZ basis is the simplest reliable approach, and we will use this description for the chemisorption studies. The orbitals of CO are shown in fig. 4b.

In the Ni_{14} cluster we find that the CO bonds to the one-coordinate site A of fig. 1 with the following geometric parameters:

$$R_{NiC} = 1.94^3 \text{ Å}, \quad R_{CO} = 1.14^6 \text{ Å}, \quad \angle NiCO = 180°.$$

The CO 5σ bonding orbital is shown in fig. 5 for $\angle NiCO = 180°$ and 140°. In fig. 6 we show the potential curve for bending the CO from the normal. As expected, the molecule prefers to be perpendicular to the surface. The orbitals are shown in fig. 4 where we see that it is the 5σ orbital (the C 2s pair) that dominates the bonding.

Table 2
Dependence of dipole moment (μ) and ionization potential on electron correlation and basis

Wavefunction	Basis	Energy (h)	Debye (μ)	Ionization potential (eV)			
				5σ	1π	4σ	3σ
HF	DZ	−112.68473	−0.530	13.57	15.32	19.90	39.70
GVB(2/4)	DZ	−112.73691	+0.052	13.05	16.14	20.12	39.87
GVB-RCI	DZ	−112.76673	+0.080	12.39	16.59	18.68	40.25
GVB-CI	DZ	−112.77585	+0.046	12.47	16.12	18.72	39.97
HF	DZd	−112.75614	−0.352	13.50	14.98	19.87	38.32
GVB(2/4)	DZd	−112.80468	+0.124	13.06	15.74	20.03	38.50
GVB-RCI	DZd	−112.83253	+0.151	12.54	16.17	18.67	38.99
GVB-CI	DZd	−112.83961	+0.139	12.59 [d]	15.78	18.72	38.94
Experimental			+0.122 [a]	14.01 [b]	16.91 [b]	19.72 [b]	38.90 [c]

[a] From ref. [15].
[b] From ref. [26].
[c] From ref. [30].
[d] 78 spatial configurations or 126 spin eigenfunctions.

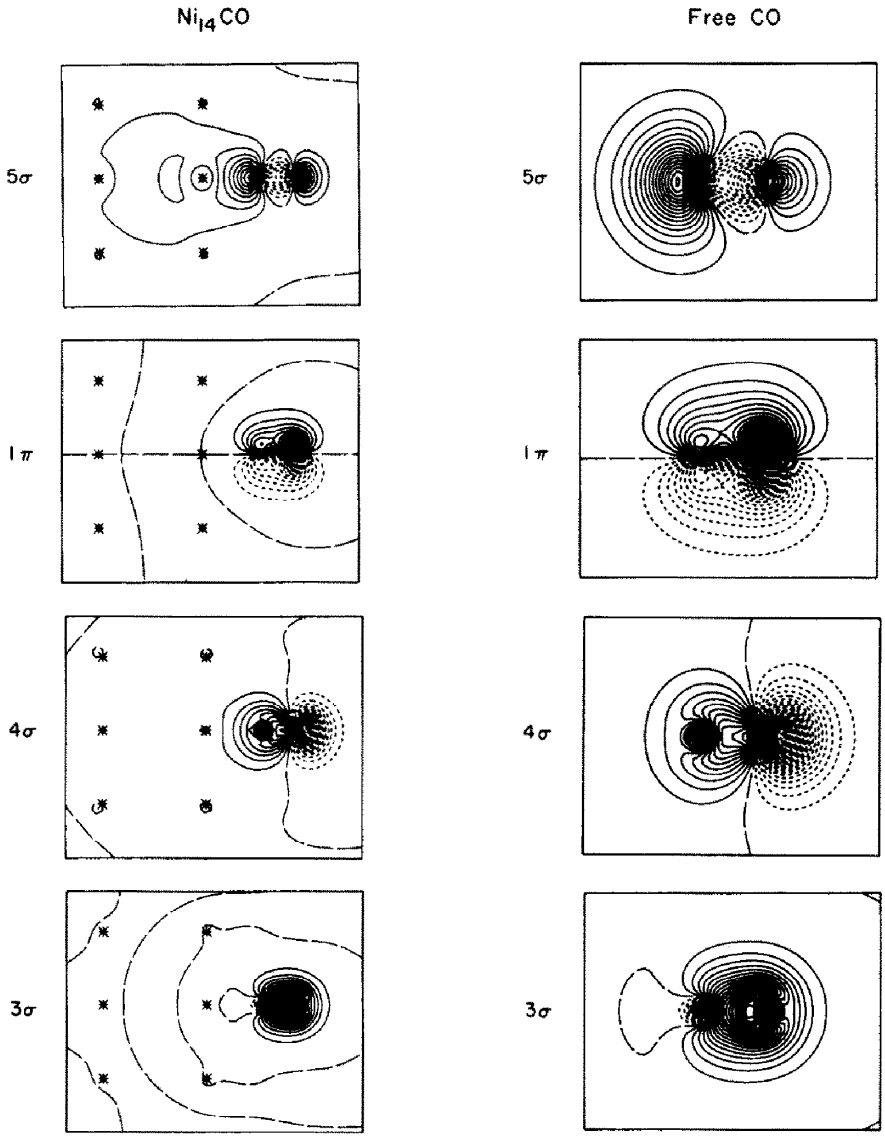

Fig. 4. Orbitals for CO [from GVB(2/4) using DZ basis]. The first natural orbital is shown for correlated pairs. The orbitals for $Ni_{14}CO$ are plotted in the $x=y$ plane (see fig. 1).

The bond energy is calculated to be

$D_e(Ni_{14}\text{-}CO) = 1.34$ eV (30.9 kcal),

which, upon correcting for zero-point energies and temperature dependence of

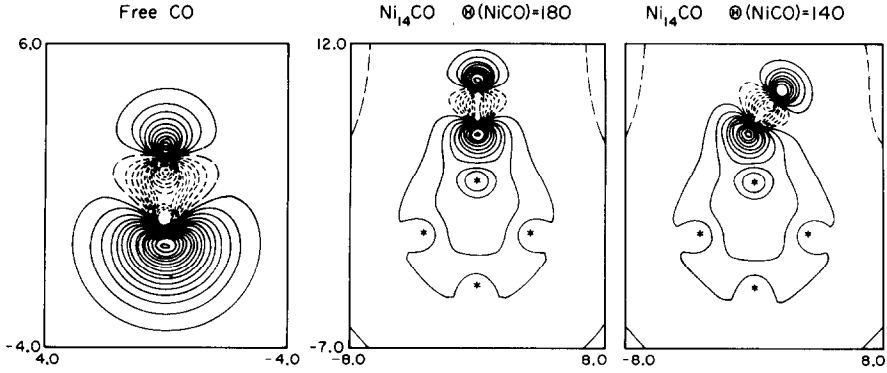

Fig. 5. The 5σ orbital of free and chemisorbed CO as a function of bond angle (plotted in the xz plane).

enthalpies, becomes *

$D_{298\,K}(Ni_{14}\text{–}CO) = 1.29$ eV (29.7 kcal).

The energy surface for calculations on $Ni_{14}CO$ is shown in table 3, and the optimum parameters for $Ni_{14}CO$ are shown in table 4.

In addition, we considered bonding of CO *backwards*; that is, with the O end toward the surface. As expected, the bond was much weaker, only 0.39 eV (8.9 kcal) rather than 1.34 eV (30.9 kcal). The optimum Ni–O bond length is 2.03 Å. Clearly, the O 2s pair does not make an effective bond to the surface. In fig. 7 we show potential curves for both $Ni_{14}CO$ and $Ni_{14}OC$.

From isosteric heat measurements for CO on the Ni(100) surface, Tracy [16] finds the heat of adsorption to be 1.30 eV for ($\theta_{CO} < 0.5$), which decreases to 1.08 eV as the CO coverage is increased ($\theta_{CO} = 0.66$). Using thermal desorption techniques (TPD mass-28 spectra), Bertolini and Tardy [5] find a bond energy of 1.30 eV for CO adsorbed on both the Ni(100) and Ni(110) surfaces. Our calculated bond energy of 1.29 eV agrees very well with these results.

In recent years there has been considerable debate as to whether molecular CO chemisorbed on Ni(001) surface stands perpendicular to the nickel surface or whether the CO molecular axis is inclined with respect to the surface normal.

Andersson and Pendry [17] examined CO chemisorbed on Ni(100) by the LEED method and proposed that the CO molecule is tipped over at an angle of $34 \pm 10°$ with respect to the surface normal. They found best agreement for a structure where the CO molecule sits directly above the Ni atom with a vertical spacing between C and O layers of 0.95 ± 0.10 Å. They explained this extremely short distance by pointing out that a displacement of the oxygen

* Assuming an ideal gas, ΔH_f and S were calculated using vibrational frequencies as discussed in section 3.2, and the calculated geometry. The symmetry number was 4.

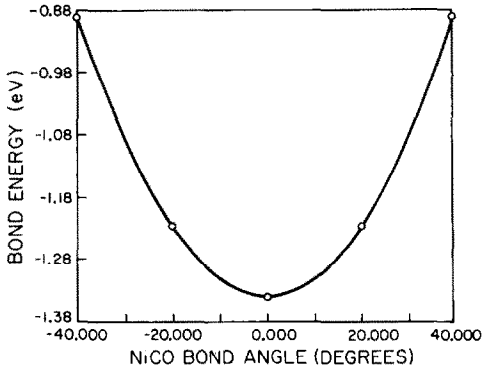

Fig. 6. The potential curve for bonding chemisorbed CO on Ni_{14}.

atom by 0.65 Å parallel to the surface, equivalent to tipping the molecule 34° away from the vertical, would increase the C–O bond length to 1.15 Å, which is the same bond length as found in $Ni(CO)_4$.

On the other hand, ultraviolet photoemission spectroscopy (UPS) results of Plummer and co-workers [18] indicate CO stands with its axis perpendicular to the (001) surface. Passler et al. [2], in an effort to resolve the inconsistency between LEED studies of Andersson [17] and the UPS studies of Plummer [18] obtained new LEED data that indicated CO stands perpendicular to the nickel surface with

$R_{CO} = 1.15$ Å, $R_{NiC} = 1.72$ Å.

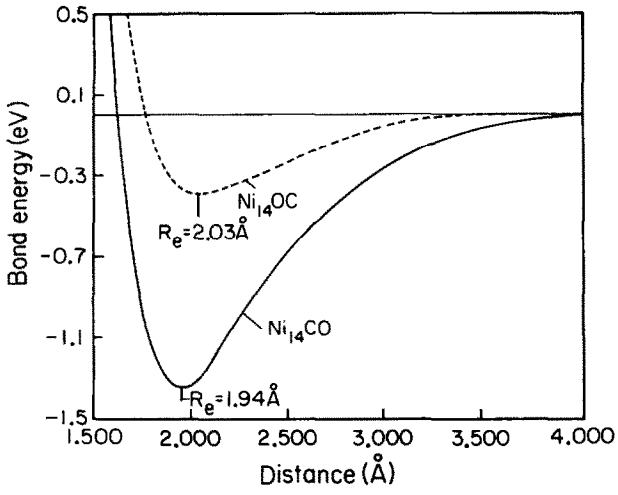

Fig. 7. The potential curve for chemisorption of CO and OC on Ni_{14}.

Table 3
Energy surface for GVB(2/4) calculations on $Ni_{14}CO$

Geometry			Energy (h)
R_{NiC} (Å)	R_{CO} (Å)	∠NiCO (deg)	
1.80	1.128	180	−117.09901
1.90	1.128	180	−117.10432
1.95	1.128	180	−117.10477
2.0	1.128	180	−117.10416
1.944 opt.			
1.94	1.13	180	−117.10477
1.94	1.16	180	−117.10508
1.94	1.19	180	−117.10173
	1.146 opt.		
1.90	1.146	180	−117.10501
1.92	1.146	180	−117.10532
1.94	1.146	180	−117.10544
1.96	1.146	180	−117.10538
2.20	1.146	180	−117.09505
3.0	1.146	180	−117.06536
5.0	1.146	180	−117.05662
1.943 opt.			
1.94	1.146	180 opt.	−117.10544
1.94	1.146	160	−117.10127
1.94	1.146	140	−117.08890

Passler also found that the only geometry for NiCO producing acceptable agreement with experimental data is the one-coordinate top-atom position. Subsequently Andersson and Pendry [3], using LEED studies, reevaluated their previous results in light of new experimental data and found their analysis was indeed consistent with a vertical C–O bond with

$$R_{CO} = 1.10 \pm 0.1 \text{ Å}, \quad R_{NiC} = 1.80 \pm 0.1 \text{ Å}.$$

Perpendicular CO adsorption has been shown to occur in other systems. ESDIAD studies confirm that CO is bonded with its axis perpendicular to the Ru(001) and W(110) surfaces as well as for Ni(111) where CO is both singly-coordinated and multiply-coordinated [19–21]. Also, Stöhr et al. have

Table 4
Optimum parameters for $Ni_{14}CO$; k is the harmonic force constant

$R_{NiC} = 1.94^3$ Å	$k = 0.4258$ h/Å$^2 = 1.8567 \times 10^5$ dyn cm^{-1}
$R_{CO} = 1.14^6$ Å	$k = 4.0634$ h/Å$^2 = 1.7716 \times 10^6$ dyn cm^{-1}
∠NiCO = 180°	$k = 2.0817 \times 10^{-5}$ h/deg$^2 = 2.9805 \times 10^{-12}$ dyn cm/rad^2

looked at Auger detection of X-ray edge features to show that CO on Ni(100) is clearly perpendicular to the surface [22].

Our calculations show that the most stable geometry for CO is perpendicular to the nickel surface with

$R_{CO} = 1.15$ Å, $R_{NiC} = 1.94$ Å.

In comparison, $Ni(CO)_4$ has experimental geometries of

$R_{CO} = 1.15$ Å, $R_{NiC} = 1.84$ Å.

Since the Ni atoms has d^{10} character in $Ni(CO)_4$ and d^9 character on the surface, we would expect *longer* NiC distances on the surface (for low coverage) and suggest $R_{NiC} = 1.9$ Å as the minimum likely geometry. The LEED experiments yield somewhat shorter NiC distances (1.72 and 1.8 Å) but this may be due to systematic errors arising from the very nonspherical nature of the orbitals on C and O and from the assumptions concerning the spherical variation in the electron–ion core potential (V_0).

3.2. *Vibrational frequencies*

The force constants for NiCO bend and the NiC and CO stretches are listed in table 5. Assuming a valence force field for a linear *xyz* molecule [23] with x = one Ni atom, these force constants give frequencies (ω_e):

49.7 meV (401 cm^{-1}) for Ni–CO stretch,

264.0 meV (2129 cm^{-1}) for CO stretch,

40.5 meV (327 cm^{-1}) for NiCO bend.

Our calculated Ni–C stretch (49.7 meV) is somewhat lower than the experimental value of 59.5 meV for CO/Ni(100) and slightly higher than the experimental value found for $Ni(CO)_4$ (46.0 meV gas, 47.1 meV solution). The calculated value for NiCO bend of 40.5 meV may help resolve the present considerable experimental uncertainty regarding this mode.

These results may be compared with those of Richardson and Bradshaw [24] who used Wilson's F and G matrix method to analyze the observed frequencies of an Ni_5CO cluster in terms of fundamental force constants. These results suggest force constants corresponding to vibrational frequencies of 54.2 meV for Ni–C stretch, 258.9 meV for C–O stretch, an NiCO bend of 50.9 meV, and a frustrated translation of 10.2 meV.

3.3. *Dipole moments*

Dipole moments have been calculated for the $Ni_{14}CO$ cluster and for free CO at the GVB(2/4) level with correlated π orbitals. For free CO we calculate a dipole moment $\mu = +0.052$ D with the negative end of the dipole pointing

Table 5

	NiC stretch		Ni–C–O bend		CO stretch	
	meV	cm^{-1}	meV	cm^{-1}	meV	cm^{-1}
Theory (ω_e) [g]						
Free CO	–	–	–	–	272.8	2200
	49.7 [f]	401 [f]	40.5 [f]	327 [f]	264.0 [f]	2129 [f]
$Ni_{14}CO$	(41.5) [e]	(335) [e]	(40.2) [e]	(324) [e]	(264.0) [e]	(2129) [e]
Experiment (ω_0) [g]						
Free CO					269.1	2143
$Ni(CO)_4$						2170 [c] (ω_e)
Gas	46.0	371 [b]	47.1	380 [d]	264.4	2132 [b]
Solution	47.1	380 [b]	47.1	380 [d]	263.5	2125 [b]
Ni(100)	59.5	480 [a]			256.4	2068 [a]

[a] From ref. [31].

[b] From ref. [32].

[c] From ref. [33].

[d] This assignment is not conclusive; see ref. [34].

[e] These values assume that the Ni cluster is rigid so that the mass of X in XCO is taken as 14 Ni atoms.

[f] Using a mass of one Ni atom in XCO.

[g] The experimental vibrational frequencies correspond to the lowest observed transition (ω_0) for the mode unless otherwise indicated. The theoretical results are for ω_e, that is, the harmonic frequencies corresponding to the force constant calculated for R_e.

towards the carbon atom. For CO adsorbed on Ni_{14} we calculate a dipole moment $\mu = 0.69$ D, with the dipole directed such that the negative end points into the cluster. Comparing these results with those obtained for free CO would indicate that the π system of CO is relatively unaffected by the nickel cluster. The major changes seem to occur in the σ system.

In recent work, Campuzano et al. [25] have related a positive work function change ($\Delta\phi \sim 1.14$ V) of a different surface [Ni(111)] to the dipole moment of adsorbed CO. They report a dipole moment of adsorbed CO to be +0.28 D with the negative end pointing *outward* from the surface.

Values of +1.1 eV and ($+0.85 \pm 0.05$) eV have been reported for the change in work function ($\Delta\phi$) for CO chemisorbed on Ni(100). As $\Delta\phi$ is positive, this implies the negative end of the dipole is pointing *outward* from the surface.

This means our results are inconsistent with the experimental results, and we may therefore conclude that small clusters do not properly describe the work function changes arising from chemisorption of CO.

3.4. Ionization potentials

The photoelectron spectrum of gas phase CO shows three low-lying peaks at 14.01 eV (5σ), 16.91 eV (1π), and 19.72 eV (4σ), where MO assignments are in parentheses [26]. However, for CO adsorbed on Ni(100) there are only two CO-derived peaks in the observed spectrum at 8.0 and 11.0 eV below the Fermi level (i.e., ~ 13.2 and 16.2 absolute IP). The 11 eV peak is assigned to the 4σ orbital, and the broad peak at 8.0 eV is interpreted in terms of overlapping 5σ and 1π derived levels [27]. These assignments imply that the 4σ–1π splitting changes only slightly from 2.8 to 3.0 eV upon chemisorption of CO, whereas the 5σ–4σ splitting is reduced from 5.7 to 3.0 eV [18,28,29]. The broad 8.0 eV peak has not been clearly resolved into 1π and 5σ components; however, angle-resolved photoemission studies have been interpreted in terms of a 5σ bonding level located (0.5 ± 0.2 eV) higher in binding energy than the 1π level (that is, the 1π and 5σ levels are reversed upon chemisorption). As shown in table 6, our calculations also lead to a reversal of 1π and 5σ upon chemisorption. We find the 5σ bonding level higher in binding energy than the 1π by 0.83 eV.

In fig. 8 are the energies of the ion states as a function of distance. Here we see that the 1π, 4σ, and 3σ ion states are all strongly bound ($D_e = 2.55$, 1.94, and 3.65 eV, respectively; $R_e = 1.85$, 1.92, and 1.80 Å, respectively); however, *the 5σ ion state is very weakly bound* ($D_e = 0.16$ eV and $R_e = 5.05$ Å). The reason for this is that the Ni–C bond is due to the 5σ orbital that interacts directly with the Ni surface. The 1π, 4σ, and 3σ states all have a doubly-occupied 5σ orbital and lead to strong, short bonds (the bond is stronger and shorter than for the ground state due to the net charge on the CO). However, the 5σ ion state has only one electron in the bonding 5σ orbital and conse-

Table 6
Ionization potentials (eV) for free CO and $Ni_{14}CO$ using GVB(2/4) wavefunctions with the DZ basis and Ni–C distance of 1.94 Å

Ion state [a]	Free CO GVB(2/4) DZ IP (eV)	$Ni_{14}CO$ IP (eV)
3σ	39.87	37.74
4σ	20.12	19.51
1π	16.14	14.95
5σ	13.05	15.78

[a] Calculated ion state is solved self-consistently.

quently makes a very weak bond. For cases such as the 1π, 4σ, and 3σ ionizations, the geometry of the ion state is similar to that of the ground state and the Franck–Condon envelope is narrow. However, since the 5σ state is dissociative, the Franck–Condon envelope is very broad. We suggest that because of this effect the observed peaks in the PES are dominated by the 1π and 4σ transitions and that the 5σ level is a very broad feature not discernible at the current level of resolution. This may explain why all cases in which associatively chemisorbed CO has been observed on single crystal surfaces lead to just the two peaks.

Other evidence that the 5σ state may be unbound comes from ESD studies.

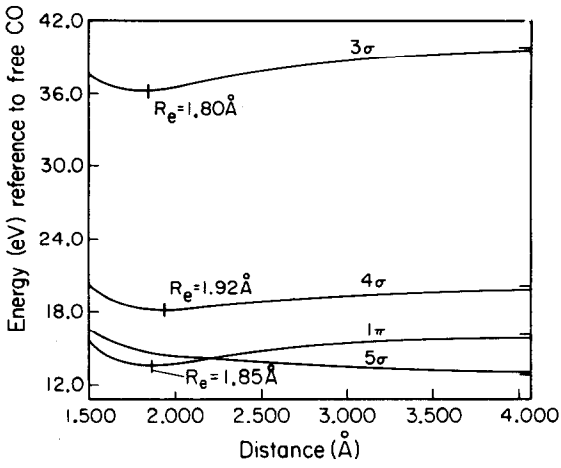

Fig. 8. The ion potential curve (5σ, 1π, 4σ, 3σ) for chemisorption of CO on Ni_{14}. Tick marks for $R=\infty$.

For CO singly-coordinated to Ni(111), CO^+ and O^+ ions are seen as desorption products; however, for bridging CO on Ni(111), only O^+ ions are seen [21]. We suggest that this may also be the case for Ni(100). Therefore, for singly-coordinated CO, the CO^+ ion yield should be most closely related to the cross section for 5σ ionizations, and we predict this would be very broad.

4. Summary

Theoretical results for CO adsorbed at the one-coordinate site of Ni_{14} and the experimental results for CO on Ni(100) are reasonably consistent for the geometry, bond energy, vibrational frequencies and ionization potentials. This provides additional support for the assumption that CO bonds to the one-coordinate site on Ni(100). In addition, these results suggest that theoretical studies using metal clusters to model bulk numbers can yield reliable results.

Acknowledgments

One of us (J.N.A.) would like to acknowledge financial support from the Fannie and John Hertz Foundation in the form of a fellowship. This work was supported in part by a grant (No. DMR79-19689) from the National Science Foundation.

References

[1] D.W. Goodman, R.D. Kelley, T.E. Madey and J.T. Yates, Jr., J. Catalysis 63 (1980) 226.
[2] M. Passler, A. Ignatiev, F. Jona, D.W. Jepsen and P.M. Marcus, Phys. Rev. Letters 43 (1979) 360.
[3] S. Andersson and J.B. Pendry, Phys. Rev. Letters 43 (1979) 363.
[4] R.L. Park and H.E. Farnsworth, J. Chem. Phys. 43 (1965) 2351.
[5] J.C. Bertolini and B. Tardy, Surface Sci. 102 (1981) 131.
[6] S. Andersson, in: Proc. 7th Intern. Vacuum Congr. and 3rd Intern. Conf. on Solid Surfaces (Vienna, 1977) pp. 815–818.
[7] F.W. Bobrowicz and W.A. Goddard III, in: Modern Theoretical Chemistry: Methods of Electronic Structure Theory, Ed. H.F. Schaefer III (Plenum, New York, 1977) Vol. 3, ch. 4, pp. 79–127.
[8] C.F. Melius, B.D. Olafson and W.A. Goddard III, Chem. Phys. Letters 28 (1974) 457.
[9] M. Sollenberger, MS Thesis, California Institute of Technology (1977).
[10] A.J.H. Wachters, J. Chem. Phys. 52 (1970) 1033.
[11] C.F. Melius, T.H. Upton and W.A. Goddard III, Solid State Commun. 28 (1978) 501.
[12] L.C. Snyder, J. Chem. Phys. 61 (1974) 747.
[13] S. Green, J. Chem. Phys. 54 (1971) 827.
[14] R. Certain and R.C. Woods, J. Chem. Phys. 58 (1973) 5837.
[15] J.S. Meutner, J. Mol. Spectrosc. 55 (1975) 490.
[16] J.C. Tracy, J. Chem. Phys. 56 (1972) 2736.

[17] S. Andersson and J.B. Pendry, Surface Sci. 71 (1978) 75.
[18] C.L. Allyn, T. Gustafsson and E.W. Plummer, Chem. Phys. Letters 47 (1977) 127.
[19] T.E. Madey, Surface Sci. 79 (1979) 575.
[20] T.E. Madey, in: Topics in Chemical Physics: Inelastic Ion–Surface Collisions, Eds. W. Heiland and E. Taglaver (Springer, Heidelberg, 1981).
[21] F.P. Netzer and T.E. Madey, J. Chem. Phys., to be published.
[22] J. Stöhr, K. Baberschke, R. Jaeger, R. Treichler and S. Brennan, Phys. Rev. Letters 47 (1981) 381.
[23] G. Herzberg, Infrared and Raman Spectra (Van Nostrand, Princeton, NJ, 1945) p. 173.
[24] N.V. Richardson and A.M. Bradshaw, Surface Sci. 88 (1979) 255.
[25] J. Campuzano, R. Dus and R.G. Greenler, Surface Sci. 102 (1981) 172.
[26] D.W. Turner, Molecular Photoelectron Spectroscopy (Wiley–Interscience, London, 1970) p. 34.
[27] R.J. Smith, J. Anderson and G.J. Lapeyre, Phys. Rev. Letters 37 (1976) 1081.
[28] T. Gustafsson and E.W. Plummer, Solid State Commun. 17 (1975) 391.
[29] A.M. Bradshaw, Surface Sci. 80 (1979) 214.
[30] T.D. Thomas, J. Chem. Phys. 53 (1976) 1744.
[31] S. Andersson, Solid State Commun. 21 (1977) 75.
[32] L.H. Jones, R.S. McDowell and M. Goldblatt, J. Chem. Phys. 48 (1968) 2663.
[33] K.P. Huber and G. Herzberg, Molecular Spectra and Molecular Structure: Constants of Diatomic Molecules (Van Nostrand–Reinhold, Princeton, NJ, 1979) Vol. IV.
[34] M. Bigorgne, in: Proc. 9th Intern. Conf. on Coordination Chemistry, Ed. W. Schneider (Verlag Helvetica Chimica Acta, Basel, Switzerland, 1966);
L.H. Jones, J. Mol. Spectrosc. 5 (1960) 133.